

# A Machine-Vision Approach to Transmission Electron Microscopy Workflows, Results Analysis and Data Management

Madeline Dressel Dukes<sup>1</sup>, Nynke Albertine Krans<sup>1</sup>, Katherine Marusak<sup>1</sup>, Stamp Walden<sup>1</sup>, Tim Eldred<sup>1</sup>, Alan Franks<sup>1</sup>, Ben Larson<sup>1</sup>, Yaofeng Guo<sup>1</sup>, David Nackashi<sup>1</sup>, John Damiano<sup>1</sup>

<sup>1</sup>Protochips, Inc.

## Corresponding Author

Madeline Dressel Dukes  
Madeline@protochips.com

## Citation

Dukes, M.D., Krans, N.A., Marusak, K., Walden, S., Eldred, T., Franks, A., Larson, B., Guo, Y., Nackashi, D., Damiano, J. A Machine-Vision Approach to Transmission Electron Microscopy Workflows, Results Analysis and Data Management. *J. Vis. Exp.* (196), e65446, doi:10.3791/65446 (2023).

## Date Published

June 23, 2023

## DOI

10.3791/65446

## URL

jove.com/video/65446

## Abstract

Transmission electron microscopy (TEM) enables users to study materials at their fundamental, atomic scale. Complex experiments routinely generate thousands of images with numerous parameters that require time-consuming and complicated analysis. AXON synchronicity is a machine-vision synchronization (MVS) software solution designed to address the pain points inherent to TEM studies. Once installed on the microscope, it enables the continuous synchronization of images and metadata generated by the microscope, detector, and *in situ* systems during an experiment. This connectivity enables the application of machine-vision algorithms that apply a combination of spatial, beam, and digital corrections to center and track a region of interest within the field of view and provide immediate image stabilization. In addition to the substantial improvement in resolution afforded by such stabilization, metadata synchronization enables the application of computational and image analysis algorithms that calculate variables between images. This calculated metadata can be used to analyze trends or identify key areas of interest within a dataset, leading to new insights and the development of more sophisticated machine-vision capabilities in the future. One such module that builds on this calculated metadata is dose calibration and management. The dose module provides state-of-the-art calibration, tracking, and management of both the electron fluence ( $e^-/\text{\AA}^2 \cdot s^{-1}$ ) and cumulative dose ( $e^-/\text{\AA}^2$ ) that is delivered to specific areas of the sample on a pixel-by-pixel basis. This enables a comprehensive overview of the interaction between the electron beam and the sample. Experiment analysis is streamlined through a dedicated analysis software in which datasets consisting of images and corresponding metadata are easily visualized, sorted, filtered, and exported. Combined, these tools

facilitate efficient collaborations and experimental analysis, encourage data mining and enhance the microscopy experience.

## Introduction

Transmission electron microscopes (TEMs) and their capabilities have benefited enormously from advances in cameras, detectors, sample holders, and computing technologies. However, these advances are hampered by disconnected data streams, limitations of human operation, and cumbersome data analysis<sup>1,2</sup>. Moreover, *in situ* and operando experiments adapt TEMs into real-time nanoscale laboratories, enabling samples to be studied in gas or liquid environments while simultaneously applying a range of external stimuli<sup>3,4,5</sup>. The adoption of such complex workflows have only magnified these limitations, and the resulting increase of the size and complexity of these data streams is an area of growing concern. Thus, there is a growing emphasis on utilizing machine-actionability to find, access, interoperate, and reuse data, a practice known as the FAIR principles<sup>6</sup>. Publishing research data in accordance with the FAIR principles concept has received favorable attention from governmental agencies around the world<sup>7,8</sup>, and application of the FAIR principles using machine-vision software is a key step in their adoption.

A machine-vision synchronization (MVS) software platform has been developed in response to the specific pain points inherent to performing and analyzing complex, metadata-heavy TEM experiments (particularly *in situ* and operando experiments)<sup>9</sup>. Once installed on the TEM, the MVS software connects, integrates, and communicates with the microscope column, detectors, and integrated *in situ* systems. This enables it to continuously collect images and align those images with their experimental metadata,

forming a comprehensive searchable database, a timeline of the experiment from start to finish (**Figure 1**). This connectivity allows the MVS software to apply algorithms that intelligently track and stabilize a region of interest (ROI), even when samples are undergoing morphological changes. The software applies adjustments to stage, beam, and digital corrections as necessary to stabilize the ROI through its **Drift Control** and **Focus Assist** functions. In addition to enriching the images with the raw metadata produced from the different experimental systems, the software can produce new, computational metadata using image analysis algorithms to calculate variables between images, which allow it to automatically correct for sample drift or changes in focus.

TEM images, and their associated metadata collected through the MVS software, are organized as an experimental timeline which can be opened and viewed by anyone *via* the free, offline version of the analysis software, Studio (hereafter referred to as the analysis software)<sup>10</sup>. During an experiment, the MVS software syncs and records three types of images from the microscope's camera or detector, which are displayed at the top of the timeline below the image viewer: single acquisition (individual single acquisition images acquired directly from the TEM software), raw (images from the detector/camera live stream that have not had any digital drift corrections applied; these images may have been physically corrected *via* stage movement or beam shift), and drift corrected (images from the detector/camera live stream that have been digitally drift). Data collected during

an experiment or session can be further refined into smaller sections or snippets of data, known as collections, with no loss of embedded metadata. From the analysis software, images, image stacks, and metadata can be directly exported into a variety of open format images and spreadsheet types for analysis using other tools and programs.

The framework of microscope control, stabilization, and metadata integration enabled by the MVS software also allows the implementation of additional machine-vision programs or modules, designed to alleviate limitations in current TEM workflows. One of the first modules developed to take advantage of this synchronization platform is electron dose calibration and spatial tracking of beam exposed areas within the sample. All TEM images are formed from the interaction between the sample and the electron beam. However, these interactions can also result in negative, inescapable impacts on the sample, such as radiolysis and knock-on damage<sup>11,12</sup>, and require a careful balance between applying a high enough electron dose to generate the image and minimizing the resulting beam damage<sup>13,14</sup>.

Although many users rely on screen current measurements to estimate the electron dose, this method has been shown to widely underestimate the actual beam current<sup>15</sup>. Qualitative dose values can be obtained *via* the screen current on the same microscope with the same settings, but reproducing these dose conditions using different microscopes or settings is highly subjective. Additionally, any imaging parameter adjustments made by the user during the experiment, such as spot size, aperture, magnification, or intensity, require a separate measurement of the screen current to calculate the resulting dose. Users must either rigorously limit the imaging conditions used during a given experiment or meticulously measure and record each lens condition used, significantly

complicating and extending the experiment beyond what is feasible for normal operation of the microscope<sup>16,17</sup>.

Dose, referred to as dose software for this protocol, is a dose calibration software module that utilizes a dedicated calibration holder designed to enable automated current measurements. A Faraday cup, the gold standard for accurate beam current calibration<sup>15</sup>, is integrated into the tip of the calibration holder. The MVS software performs a series of beam current and beam area calibrations for each lens condition and embeds those values on the images at the pixel level.

In this video article, MVS software protocols designed to enhance all areas of the TEM workflow are presented using representative nanomaterial samples. A beam sensitive zeolite nanoparticle sample<sup>14</sup> is used to demonstrate the calibration and dose management workflows. We perform a representative *in situ* heating experiment using an Au/FeO<sub>x</sub> nanocatalyst<sup>18,19</sup> sample that undergoes significant morphological changes when heated. This *in situ* experiment highlights the software's stabilization algorithms and its ability to collate multiple streams of metadata, which is an inherent challenge for *in situ* and operando studies. Although not described in the protocol, because of its unique electron dose sensitivity, we discuss representative examples of the software's utility for liquid-EM studies (protocols for which have been previously reported in the literature<sup>20,21,22</sup>), and how these techniques can be applied to improve the understanding of the effect of dose on liquid-EM experiments. Finally, we show how data analysis is streamlined using the offline analysis software to visualize, filter, and export a variety of image, video, and data files into other accessible formats.

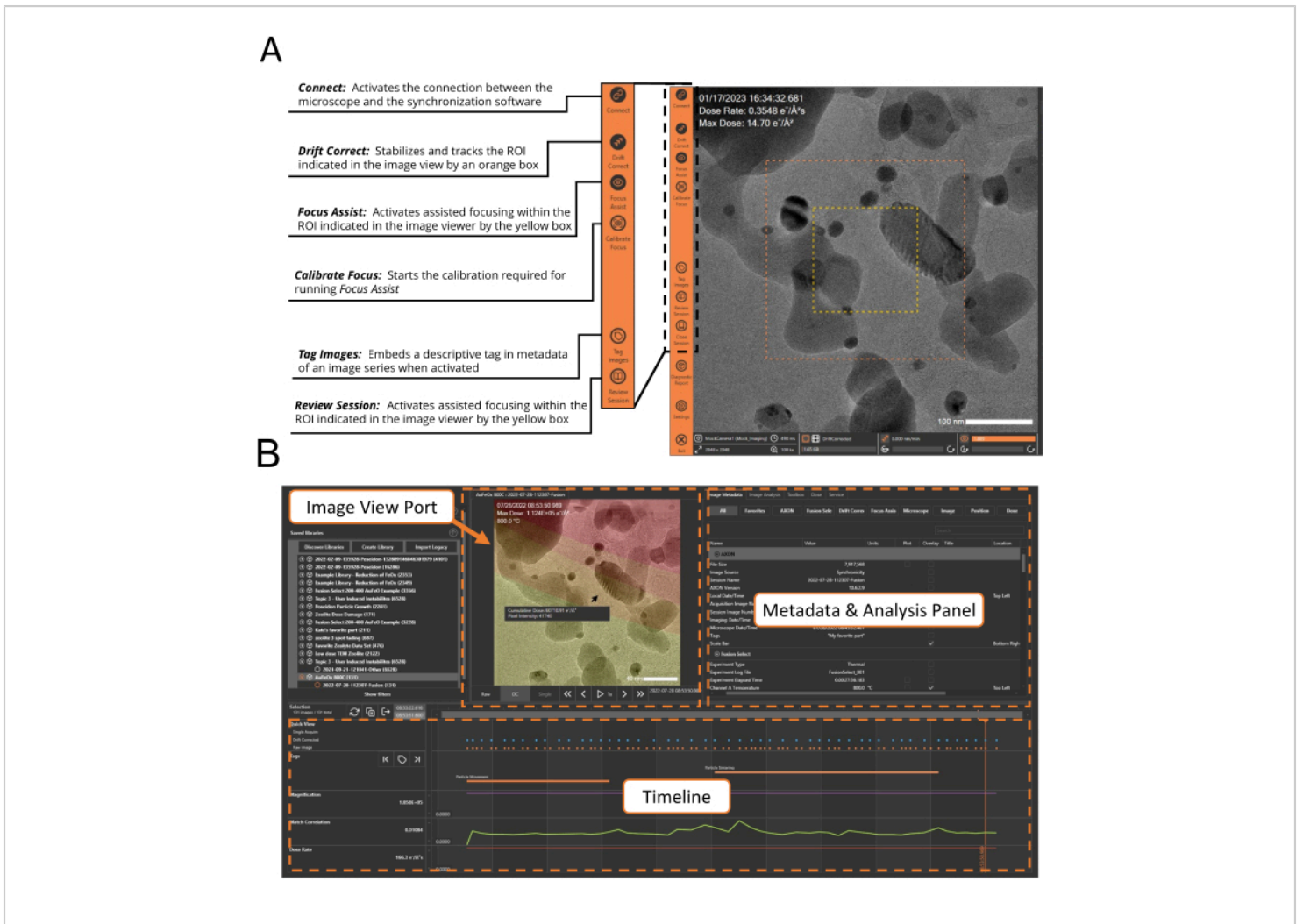


**Figure 1: User interface examples for MVS and analysis software. (A)** The synchronization software image viewing pane and control panel. A connection between the TEM and the synchronization software is established by activating the **Connect** button, which streams the images and metadata from the microscope into the synchronization software. From the image viewer, the operator can perform a variety of machine-vision assisted operations, such as **Drift Correct** and **Focus Assist**. It also provides the ability to apply **Tag Images** and **Review Session** without disrupting data collection. **(B)** Screenshot of the image analysis software highlighting the location of the **Image View Port**, **Timeline**, and the **Metadata and Analysis** panel. The analysis software can be accessed at any point during an experiment to review the images acquired up to that time point using the **Review Session** button. [Please click here to view a larger version of this figure.](#)

## Protocol

### 1. Method 1: Dose calibration of the transmission electron microscope for TEM and scanning TEM (STEM) imaging modes

1. Turn on the picoammeter and allow it to warm up for a minimum of 30 min before starting a dose calibration. Load the dose calibration holder into the TEM and connect the calibration holder to the picoammeter using the quick-connect cable.

2. With the microscope in **TEM** mode, open the column valves and locate the 35  $\mu\text{m}$  fiducial hole on the dose holder (**Figure 2**). Launch the MVS software application and select **Dose (Calibration Automation)** from the experiment options.

**NOTE:** The fiducial hole location is saved by the software after the initial calibration, enabling the software to automatically locate its position for future calibrations.

3. Click on the **Connect** icon (**Figure 1A**) and select the microscope to activate the connection between the TEM and the MVS software. Once connected, the images from the camera/detector will be visible in the image viewer of the software.

**NOTE:** It is not necessary to optimize the eucentric height, and the edge of the fiducial hole may appear blurry due to the thickness of the tip. This will not affect the current measurements.

4. Navigate to the **Dose** tab and then to **Dose Calibration**. Select **Dose Area Calibration** process, follow the software prompts, and enter the requested user-configurable values (such as the aperture and monochromator settings). After the **Dose Area**

**Calibration** is complete, select the **Dose Current Calibration** process and follow the software prompts.

5. Repeat the calibration process (step 1.4) for each spot size, aperture, or monochromator setting that may be utilized during the experiment.

6. When the calibration process for **TEM** mode is finished, calibrate the electron dose for **STEM** mode by repeating step 1.4.

**NOTE:** STEM mode does not require the **Dose Area Calibration** to be performed.

7. When all desired calibrations are finished, click on **Close Session**, remove the dose calibration holder, and return to the start screen of the MVS software.

### 2. Method 2: Determination of dose threshold using the MVS and dose software

1. Load a standard TEM grid with a sample (commercially available ZSM-5 zeolite nanoparticles were used in this example) into a standard TEM holder. Insert the holder into the TEM and locate a region of interest (crystalline zeolite nanoparticles).

2. Open the MVS software application and select **Other**.  
**NOTE:** Additional information about the sample (e.g. sample identifier and description, the operator name, and experiment notes) can be added to the experimental parameters field.

3. Repeat step 1.3 to connect to the MVS software and navigate to the image metadata tab in the MVS software interface to select the following metadata to overlay on the image stream shown in the live display: **Magnification**, **Max Dose**, and **Dose Rate**. Other metadata may be included if the user desires. A screenshot of the MVS software interface

showing the dose management controls is provided in **Supplementary File 1**.

4. Open the **Dose** tab and select **Dose Management** and **Enable Dose Monitoring** to activate automated electron dose tracking. Select **Show Dose Layer** to display the dose color overlay.
5. Set the values for the high dose level and the high dose rate and press on **Save** (in this example, values of 60,000  $e^-/\text{\AA}^2$  and 500  $e^-/\text{\AA}^2 \cdot \text{s}$ , respectively, were used).
6. Navigate to the **Settings** tab, select **Dose**, and set the **Dose Navigation Map Opacity** and **Dose Image Overlay Opacity** values (in this example, values of 0.50 and 0.30, respectively, were used).
7. In the **Live Image Viewer** window, activate drift correction by clicking on **Drift Correct**.
8. Navigate to the **Data View** tab and plot the metadata values **Defocus** and **Focus Quotient** on the Y axis.  
**NOTE:** Any of the available metadata values can be plotted in real time during the experiment from the data view table.
9. Activate **Focus Assist**, and then select **Calibrate Focus** to run the automated focus assist calibration. Once the **Calibrate Focus** routine is complete, close the **Data View** tab.
10. Open the **Image Analysis** tab in the MVS software and activate the **Live FFT** and **Quadrants 1 & 2** options.
11. Using the microscope's software controls, adjust the beam conditions so that the electron flux is  $\sim 500 e^-/\text{\AA}^2 \cdot \text{s}$ . and move to a new region in the sample and center the sample ROI in the live view of the MVS software.

**NOTE:** When making large stage movements, drift control and focus assist will automatically de-activate, and must be re-engaged once the new ROI is selected.

12. Make a note of the dose conditions in the software using the **Tag** function. Highlight the **Tag** icon and enter the desired text to denote a specific series of images within the timeline. Images will be tagged with this text until the **Tag** icon is deselected.
13. Maintain a constant dose rate while continuously imaging the same ROI until the peaks corresponding to the atomic structure in the FFT plot have disappeared.
14. Reduce the magnification, open the **Dose Management** tab, and activate **Show Dose Layer** to overlay a color-coded dose map.  
**NOTE:** This feature provides a visual reference of the areas of the sample that have been exposed to the electron beam and their relative dose exposure. Highlighting these areas in individual images with the cursor will indicate their respective dose values.
15. Disconnect and end the session by deselecting **Connect**, then select **Close Session**. Save a copy of the session data to an external source to prevent the data saved in the MVS software from being overwritten during subsequent experiments (**Supplementary File 2**).

### 3. Method 3: Metadata and trend analysis and data export using the analysis software

1. Launch the analysis software (the offline software for viewing the fully synchronized datasets) and open the experiment session file by selecting it from the file library.  
**NOTE:** Users can also access the analysis software through the **Review Session** icon in the MVS software during an experiment.

2. Display the drift corrected images by activating the **DC** tab below the **Image View Port** and select the desired data overlays by checking their respective **Overlay Data** boxes in the **Image Metadata** tab (in this example **Microscope**, **Date/Time**, **Dose Rate**, **Max Dose**, and **Magnification** were used). Other metadata may be plotted as the user desires.
3. Check the **Timeline** box for **Max Dose** and **Dose Rate** to add a graphical plot of these values to the timeline. Highlight or scroll through these graphical plots to update the image displayed in the viewport. Access a variety of tools through the **Notes**, **Image Analysis**, **Toolbox**, and **Data View** tabs.
  1. Access the FFT for each image through the **Image Analysis** tab and click on **Live FFT** to update the FFT while scrolling through images.
  2. Use the fading of the FFT peaks to determine the time point at which the zeolite structure loses crystallinity. Record the max dose value recorded with that image.
4. Use the **Filter** option to filter large datasets easily into smaller, sharable datasets without losing their associated metadata. Open the filter panel and adjust the sliders so that only data with a dose rate equal to or above  $\sim 500 \text{ e}^- / \text{\AA}^2 \cdot \text{s}$  is selected, and save the new collection using the name **Dose Threshold Study**.
 

**NOTE:** Filters may be applied for any of the associated metadata types.
5. Export the images and metadata from the session into other file types enriched with scale bars and metadata overlays.
  1. Highlight the collection in the library pane and select **Publish** by right-clicking the selection. From the **Publish** window, select the desired options for the file type export.
  2. Select the drift corrected data tab and apply overlays of any desired metadata and the FFT (position the FFT overlay as desired; examples of images exported with the FFT are shown in **Figure 3**).
6. Export the image series as a movie file using the same **Publish** option. Select the images by highlighting them in the timeline, using the filter options or exporting the full database file. Select the desired movie format, frame rate, and file location. A movie of the zeolite degradation experiment obtained using a 200 kV TEM is provided in **Supplementary File 3**.
7. Export the metadata separately from the acquired images as a CSV file by selecting the **Metadata (CSV)** option while publishing.
 

**NOTE:** Raw and drift corrected images are exported as separate CSVs (**Supplementary File 4** and **Supplementary File 5**).

#### 4. Method 4: *In situ* heating study of gold on iron oxide nanoparticles

1. Dropcast a nanocatalyst ( $\text{Au}/\text{FeO}_x$ ) suspended in ethanol onto an *in situ* heater E-chip, a micro-electrochemical (MEM) sample support, and allow it to air-dry. Mount the sample in the *in situ* heating holder, insert the holder with the sample into the TEM, and connect the holder to the power supply using the supplied cable. Locate a sample ROI using the TEM controls.

**NOTE:** This experiment used a heating holder which is fully integrated with the MVS software, enabling temperature metadata to be embedded with the images.

2. Select the appropriate workflow option from the MVS software (in this example, the **Fusion Workflow** was used, but other manufacturer heating holders can be used by selecting **Other**).
3. Follow the workflow prompts to confirm the electrical connection between the holder and the heating E-chip by loading the calibration file and performing a device check.
4. Connect the microscope to the MVS software, as shown earlier in steps 2.3-2.10 (in this example, the metadata values for dose rate, max dose, match correlation, drift rate, and channel A temperature were selected), and center the sample ROI in the field of view.
5. Open the **Fusion AX** tab and set up and apply a temperature.
6. Click the **Channel A Setup** button to access the temperature control settings. Select the **Temperature** function and **Manual** control mode.
7. Click the **Experiment** button to access the experimental controls. Set the **Ramp Rate** to 10 °C/s and the **Target** to 600 °C. Click on **Apply** to start the experiment.

**NOTE:** The experiment can be paused or stopped at any time using the quick access buttons in the bottom right corner of the MVS software, without opening the **Fusion AX** tab.

8. After the set temperature of 600 °C is reached, open the **Fusion AX** tab and select **Experiment**. Change the **Ramp Rate** to 2 °C and the **Target** to 800 °C. Click on **Apply** to start the experiment.

**NOTE:** The procedure for applying a heating ramp is dependent on the *in situ* heating system that is used. The

steps highlighted above to apply the temperature ramp apply to the system used in this example.

9. Highlight any events or points of interest during the experiment using the tagging feature, as shown in step 2.10. Continue to image the sample and adjust the temperature profile as desired. When finished, click on **End Session** and save the data file using the analysis software (a portion of the database file discussed in the representative results is supplied as **Supplementary File 6**).
10. Open the analysis software to review the session. Plot the temperature, template morphing factor, dose rate, and cumulative dose in the timeline. Export images and movies as desired using the steps outlined in step 3.6 and 3.7. Images and movies may be exported with or without the dose map overlays (**Figure 4**).

## Representative Results

This work highlights the utility of data acquisition using MVS software for TEM imaging and *in situ* experiments. Microscope alignment and condition setup were performed and selected through the TEM manufacturer's default controls. After initial setup, the protocols presented in this video article were conducted through the MVS software. A 300 kV TEM was used for all experiments presented in the video protocol and representative data, except for the comparison zeolite data which was acquired using a 200 kV cold FEG (**Figure 3D-F** and **Table 1**). All metadata was collected and aligned to its respective images automatically by the MVS software.

After launching the software and selecting the appropriate workflow from the menu, a connection to the microscope is established by activating the **Connect** button in the toolbar

in the far left of the image viewer, as shown in **Figure 1A**. When the **Connect** button is highlighted, images and associated metadata from the microscope are automatically streamed into the MVS software and appear in the image view pane. These images and their associated metadata are saved chronologically in a timeline that can be opened, reviewed, and analyzed without interrupting the recording of new data into the timeline (**Figure 1B**). Streaming can be interrupted by the user at any time by deactivating the **Connect** icon.

Once the connection is activated, other workflows that are dependent on the MVS software framework can be accessed. In the examples shown in this video protocol, a dose calibration must be performed before utilizing the other functions of the MVS software. Dose calibration is an automated process controlled by the MVS software; it uses a dedicated Faraday cup dose calibration holder to measure the beam's current and area for the combination of parameters. The Faraday cup calibration holder, shown in **Figure 2**, connects to an external picoammeter, which precisely measures the beam current. Once inserted in the microscope, the fiducial alignment hole is centered and the desired beam conditions to be calibrated (spot sizes, apertures, and magnifications) are entered in the software. The software performs a series of calibration steps for each combination of the selected conditions. During dose calibration, the holder automatically moves between the integrated Faraday current collector cup and the through-hole. The current measurement for each combination of lens conditions is measured on the Faraday cup by the picoammeter. Then, the software translates the stage to center the beam in the through-hole and the beam area is determined through machine-vision algorithms. This series of measurements builds a profile of the relationship between the intensity/brightness and the beam area. This

enables the software to extrapolate the beam area as the intensity/brightness setting is adjusted during an experiment regardless of the field of view. Values for cumulative dose and dose rate are calculated using these beam current and beam area measurements and a dose calibration file is generated. This process essentially defines a dose "fingerprint" for the TEM and its individual lens conditions. Once the dose is calibrated for the TEM, the user is able to operate normally and freely adjust the magnification and intensity with no loss of dose information or manual note taking<sup>17</sup>. After calibration is complete, the dose calibration holder is removed, allowing the sample to be inserted as normal. The calibration process for both the TEM and STEM modes normally takes less than 10 min.

After calibrating the dose conditions, a commercially purchased zeolite nanoparticle (ZSM-5) sample was imaged under high dose rate conditions to determine the threshold (cumulative) dose at which the sample is too damaged to provide structural information. The ZSM-5 nanoparticles were suspended in ethanol and dropcast on a conventional copper TEM grid. They were imaged continuously at 300 kV in TEM mode using a spot size of 3 and a 100  $\mu\text{m}$  condenser aperture. The dose rate read by the MVS software under high dose rate conditions was  $519 \text{ e}^-/\text{\AA}^2 \cdot \text{s}$ . Nanoparticles in the field of view were imaged continuously until the peaks in the FFT disappeared, indicating degradation of the crystalline structure, as shown in **Figure 3A-C** and **Supplementary File 3**. Overlays (which can be added during a live experiment or afterward in the analysis software) were applied to the TEM images to show the date and time, dose rate, maximum (cumulative) dose, and magnification. The dose rate was kept constant during experiments, with the cumulative dose (max dose) increasing as a function of time. The FFT peaks began to disappear after 42 s of continuous imaging (**Figure 3B**). At

1 min and 20 s and a cumulative dose of  $\sim 60,000 \text{ e}^-/\text{\AA}^2$ , the FFT peaks had completely disappeared (**Figure 3C**).

To show that this calibration method generates quantitative dose measurements that can be applied to other microscopes operating under different settings, the same calibration process and zeolite degradation experiment was conducted using a 200 kV cold field emission gun (FEG) TEM and a spot size of 1. This microscope was calibrated using the same procedure described in Method 1, and the same experiment described in Method 2 was performed using the new spot size and aperture settings. The beam settings were adjusted so that the difference in the applied dose rate between the two experiments was negligible ( $499 \text{ e}^-/\text{\AA}^2 \cdot \text{s}$  vs.  $519 \text{ e}^-/\text{\AA}^2 \cdot \text{s}$ ). As shown in **Figure 3D-F** and summarized in **Table 1**, the FFT spots fully disappear after 1 min and 50 s of continuous imaging and a cumulative dose of  $58,230 \text{ e}^-/\text{\AA}^2$ , which aligns with the values obtained in the first experiment.

An example of how the MVS software can benefit *in situ* experiments was shown by performing a heating experiment. A representative nanocatalyst sample, Au/FeO<sub>x</sub> (synthesized following a published procedure<sup>19</sup>), was selected as an example system because it undergoes dynamic morphological and structural changes at high temperatures. This temperature-induced mobility makes it

challenging to keep the ROI centered within the field of view due to the sample's own movement and thermal expansion of the sample support itself during temperature changes<sup>18</sup>. With the **Drift Correct** and **Focus Assist** features enabled, the sample was imaged over a period of  $\sim 30 \text{ s}$  at  $800 \text{ }^\circ\text{C}$ . At elevated temperatures, the gold nanoparticles within the Au/FeO<sub>x</sub> migrated along the surface of the iron oxide support and sintered to form larger particles, as shown in **Figure 4** and as a movie in **Supplementary File 7**. **Figure 5** shows a series of TEM snapshots (**Figure 5A-F**) of a porous region within an Au/FeO<sub>x</sub> nanocatalyst, recorded at various time points (**Figure 5G**) during an *in situ* heating experiment. The coordinated drift value of the ROI was automatically calculated by the software. The coordinated drift and temperature values of the images over the course of the series is shown graphically in **Figure 5G**. As expected, the coordinated drift of the sample increases as the temperature profile increases, from a rate of  $\sim 9 \text{ nm/min}$  to  $\sim 62 \text{ nm/min}$ , and begins to decrease toward leveling off as the temperature is held constant. Despite this high rate of drift, and changes to the sample's morphology, high resolution images are easily obtained during temperature ramping, revealing movement within the porous region, as shown in **Supplementary File 8**. Refer to **Supplementary File 9** for download instructions and computer specifications.

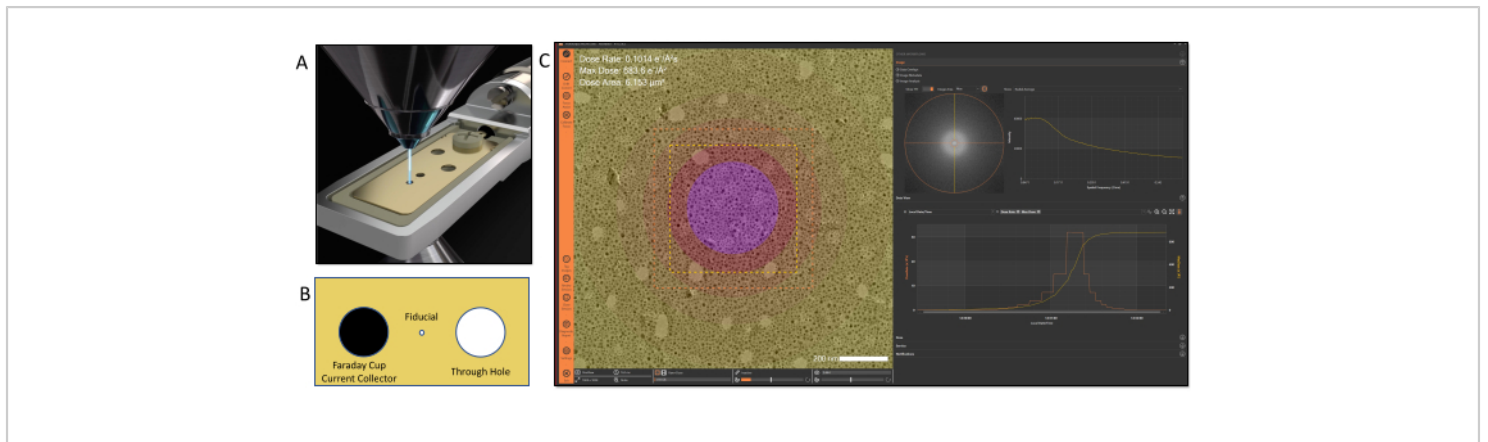


**Figure 2: Electron dose calibration and tracking.** (A) Dose is calibrated using a dedicated sample holder that contains a current collector positioned at the sample plane for beam current measurements. (B) Illustration of the features of the tip design: Left: Faraday cup; Middle: fiducial hole; Right: through hole (C). The applied electron dose can be visualized in the software using color-coded maps to denote different dose exposures within an image. [Please click here to view a larger version of this figure.](#)

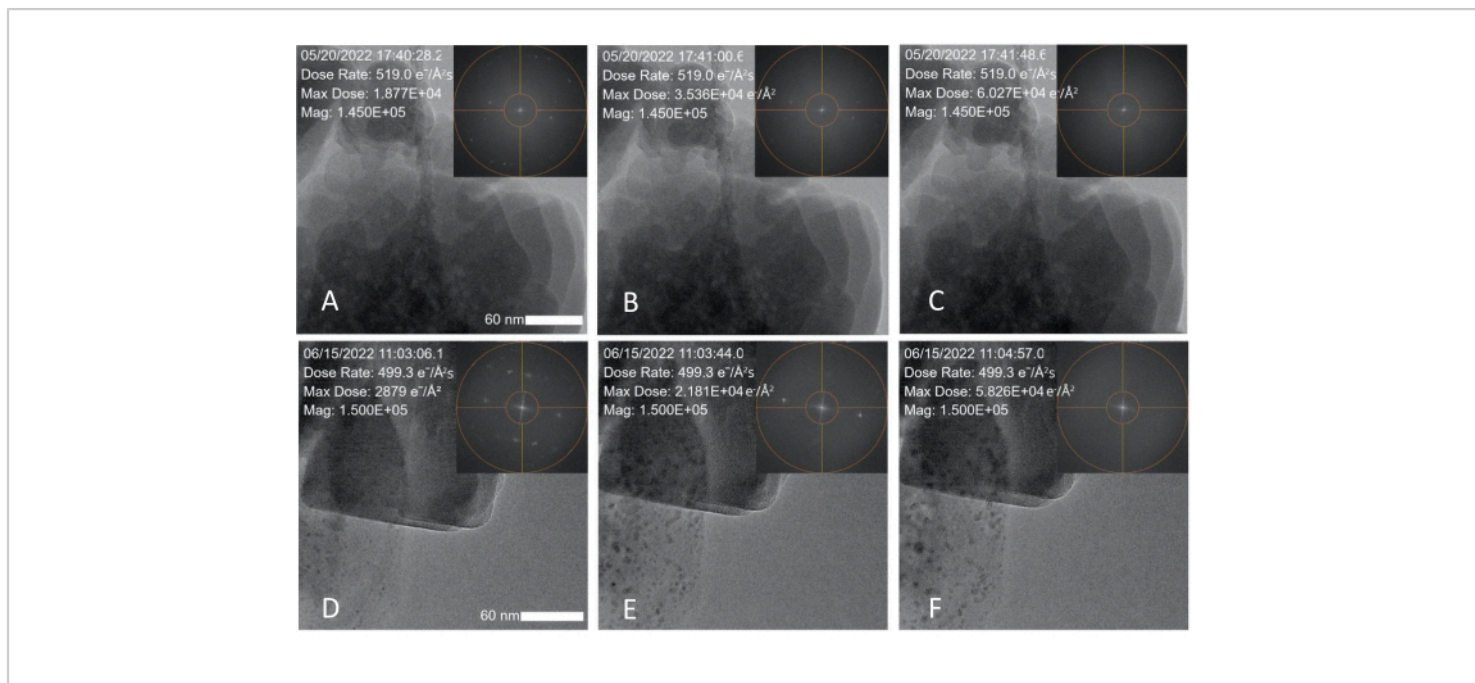


**Figure 3: Electron dose induced degradation of zeolite (ZSM-5) nanoparticles.** (A-C) Snapshots taken over a 1 min and 20 s period showing degradation data obtained with a 300 kV FEG and a measured dose rate of 519 e<sup>-</sup>/Å<sup>2</sup>·s; the zeolite degrades within 1 min and 20 s. (D-E) Snapshots taken over a 1 min and 50 s time period showing degradation data obtained with a 200 kV cold FEG TEM and an electron dose rate of 499 e<sup>-</sup>/Å<sup>2</sup>·s; the insets show the FFT spot fading over time. The scale bar is 60 nm. [Please click here to view a larger version of this figure.](#)

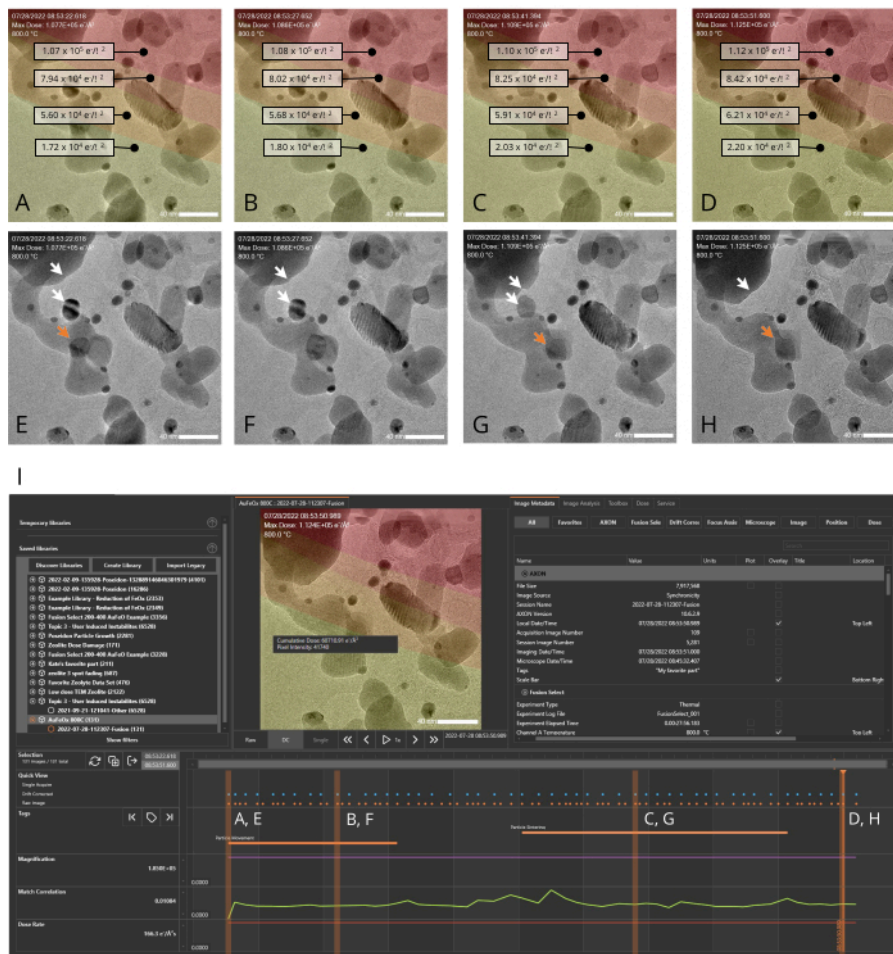


**Figure 4: AXON synchronicity applies machine-vision algorithms to track and stabilize dynamically evolving samples.** Metadata generated during the experiment can be plotted along the timeline, allowing the user to quickly pair an image with its associated metadata as they scroll through the image series generated during the experiment. (A-H) Images of a nanocatalyst sample ( $\text{Au}/\text{FeO}_x$ ) at  $800^\circ\text{C}$  recorded over a period of 28 s both with (A-D) and without (E-H) the dose map overlay. Red areas in the overlay indicate regions of high cumulative dose exposure, and yellow areas indicate regions of lower exposure. Highlighting an individual pixel indicates the cumulative dose for that pixel. White arrows in panels E-H indicate two particles that merge during the experiment, and the orange arrow indicates the trajectory of a moving gold particle. (I) The experiment timeline generated by the analysis software for the image series shown in A-H. The orange dots at the top of the timeline denote raw (non-digitally corrected) images and the blue dots denote drift corrected images. The orange vertical bars indicate the points on the timeline corresponding to the images shown panels A-H. The scale bar is 40 nm. [Please click here to view a larger version of this figure.](#)

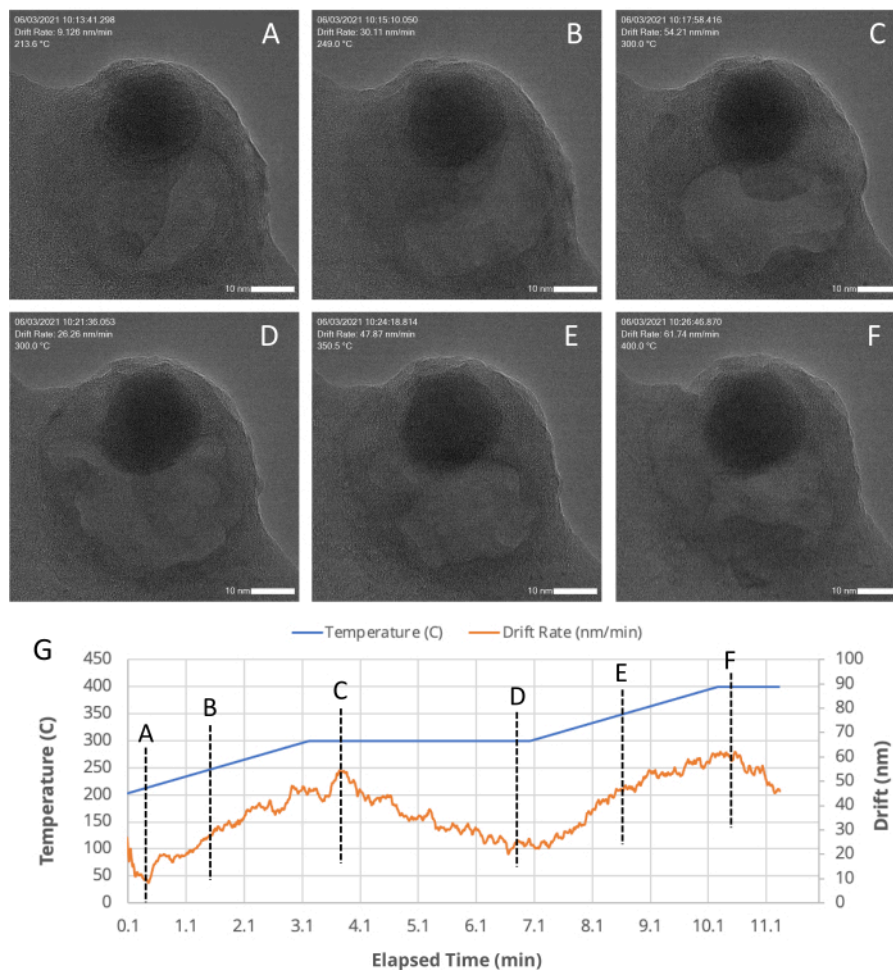


**Figure 5: TEM snapshots of a porous region within an Au/FeOx nanocatalyst at various time points.** The MVS software stabilizes and centers the sample even during high drift rates, such as those that occur during a temperature ramp through the application of stage, beam shift, and digital corrections, as indicated by machine-vision algorithms. (A-F) TEM snapshots of a porous region within an Au/FeOx nanocatalyst, recorded at various (G) time points during an *in situ* heating experiment. The drift rate of the ROI is automatically calculated and recorded during an experiment by the MVS software. As plotted in (G), as the temperature profile is changed (the blue line), the drift rate (orange line) increases as the temperature increases and decreases as the temperature is held constant. [Please click here to view a larger version of this figure.](#)

| Microscope Type   | 300 kV FEG TEM                                | 200 kV Cold FEG TEM                           |
|---|---|---|
| Spot Size/Condenser 2 Aperture                          | 3/100 $\mu\text{m}$                           | 1/100 $\mu\text{m}$                           |
| Dose Rate   | $519 \text{ e}^-/\text{A}^2 \cdot \text{s}^1$ | $499 \text{ e}^-/\text{A}^2 \cdot \text{s}^1$ |
| Loss of Structure Measured by FFT<br>(Accumulated Dose) | $60,270 \text{ e}^-/\text{A}^2$               | $58,230 \text{ e}^-/\text{A}^2$               |

**Table 1: Summary comparison of zeolite degradation results obtained from different microscopes.**

**Supplementary File 1: Screenshot of the MVS software interface with the dose management tab open.** [Please click here to download this File.](#)

**Supplementary File 2: MVS software database file of the beam-induced zeolite degradation experiment.** This viewing/analysis software is available to download for free. Please see **Supplementary File 9** for download instructions and computer specifications. [Please click here to download this File.](#)

**Supplementary File 3: Movie of the beam induced zeolite degradation.** [Please click here to download this File.](#)

**Supplementary File 4: CSV file 1 (zeolite degradation: raw data [mechanical correction only])** [Please click here to download this File.](#)

**Supplementary File 5: CSV file (zeolite degradation: drift corrected [mechanical + digital correction])** [Please click here to download this File.](#)

**Supplementary File 6: MVS software database file nanocatalyst *in situ* heating experiment.** [Please click here to download this File.](#)

**Supplementary File 7: Movie of the nanocatalyst at 800 °C with dose overlays.** [Please click here to download this File.](#)

**Supplementary File 8: Movie of the nanocatalyst during a temperature ramp with coordinated drift values.** [Please click here to download this File.](#)

**Supplementary File 9: Instructions for downloading the free analysis software.** [Please click here to download this File.](#)

## Discussion

The interpretation of TEM experimental results is often contingent on many inter-connected experimental parameters, such as microscope settings, imaging conditions, and in the case of operando or *in situ* experiments, changes to the environment or stimuli<sup>1,23</sup>. Accurate analysis of large TEM datasets, over which these parameters may be continuously modified, requires significant attention from the operator to accurately record each condition and setting for each image in a lab journal or other external documentation

source. As TEM datasets grow in size and complexity, manual recordkeeping becomes unmanageable, and key information may be missed or inaccurately recorded. The MVS software described here consolidates the metadata generated during an experiment from the microscope, the detector/camera, and other systems (such as *in situ* sample holders) and aligns them with their respective images.

In addition to metadata consolidation, the software applies machine-vision algorithms to track and stabilize the field of view through a combination of spatial, beam, and digital corrections using its **Drift Correct** and **Focus Assist** functions. When the **Drift Correct** function is engaged, a cross-correlation 'template' image is generated using the first image pulled into the MVS software. The template is then compared to incoming images to calculate the direction and magnitude of the sample drift or movement. With this information, the MVS software automatically applies the necessary corrections to keep the image features in the same place by adjusting at least one of three parameters: stage location, beam or image shift, and digital image correction. The **Focus Assist** function utilizes a combination of algorithms to assign a focus value, called the focus score to each image, and those scores are compared to determine the magnitude and direction of defocus adjustment to apply to keep the sample in focus. In STEM imaging mode, the MVS software attempts to maximize contrast through a proprietary version of normalized variance to assign the focus score. In TEM mode, a radial sum of intensity is calculated in the FFT and used to calculate the focus score. Limitations to the MVS software's ability to optimize the focus occur when it cannot accurately calculate the correct focus score for an image. This typically occurs when the microscope is misaligned or the sample is significantly out of focus during calibration, preventing the software from correctly calculating

the correct starting focus score value. The MVS software can have difficulty calculating the focus score for samples with well-defined lattice fringes, as the lattice fringes in the FFT can 'overwhelm' the focus scoring algorithm; thus, if a sample moves out of focus, the focus score may not accurately reflect the change in focus. Conversely, working at low magnifications or with a sample that has a low FFT signal can also make it challenging to calculate a good focus score. To mitigate these difficulties, the MVS software contains a number of additional algorithms that can be selected by the user for calculating the focus score if the default settings are unsuitable for the sample. These must be tested and applied on a case-by-case basis to determine the best algorithms for a given experiment.

Morphological changes in the sample structure over time are accounted for using a template morphing factor. This filter is tunable by the operator, so that registration algorithms account for morphological changes over time. Additionally, the software monitors the continuous image, microscope settings, and camera or detector settings to automatically update the template when triggered by changes in sample structure and after any operator-induced changes to the microscope, camera, or detector parameters. As shown in **Figure 4**, **Figure 5**, **Supplementary File 7**, and **Supplementary File 8**, the MVS software provides effective, immediate stabilization, allowing high resolution imaging of dynamically moving or changing samples. Although the software is capable of controlling very high rates of drift or sample movement, such as those that occur when applying a heating ramp during an *in situ* experiment, there are limitations to the maximum stage corrections or beam shifts that the software can control if the sample is moving or drifting very rapidly. This limit is a function of the image update rate, field of view size, and drift rate. For a given field of view and

image update rate, there is a maximum drift rate that can be corrected, and if the physical movements cannot keep up, then the process may end or become unstable. From the registration templates generated when features such as **Drift Correct** are applied, additional calculated metadata can be generated. For instance, **Match Correlation** is a numerical record of the extent of change between templates in a series and is used to identify points in an experimental timeline in which the sample changed. A high match correlation value corresponds to a sample that has undergone changes to its morphology, and a low match correlation value corresponds to a sample whose structure remains relatively static. Match correlation is particularly valuable for *in situ* studies as it can be plotted graphically, enabling the user to quickly pinpoint images in the series corresponding to significant sample change. It is important, however, to understand that high match correlations values can also correspond to changes in imaging conditions, such as moving the stage or changing the magnification, if these actions are performed while the **Drift Correction** function remains active.

The calibration workflow presented here utilizes a unique calibration holder and a semi-automated calibration routine to accurately calibrate the beam under a variety of lens conditions with minimal operator intervention. The dose calibration routine is accessed through the MVS software installed on the TEM. The MVS software automatically reads the relevant microscope settings to save all measurements to reference for later experiments. On some TEMs, it is not possible to read the aperture or monochromator settings, and these must be entered into the MVS software settings by the operator during calibrations and during use. There are reminders built into the software to help keep these operator input settings updated by following the program prompts. The development of a holder with a built-in current collector, rather

than relying on one integrated elsewhere in the microscope column, is a deliberate design choice. This enables the current collector to be positioned at the same plane as a sample, eliminating errors in the current measurement caused by beam deflection or differences in the absorption of electrons by apertures at different beam positions. The MVS software follows an automated routine to measure the beam current and area for any combination of lens conditions. The software can then correlate these measured calibrations with the camera or screen current and extrapolate any changes in magnification etc. to the beam area during the experiment. Once generated, these calibration files can be used immediately and are automatically saved for later use if the software detects the same settings being used during a future session. Although the longevity of the calibration file varies from microscope to microscope, the authors have found that they are able to use the same calibration files for several months without observing substantial changes to the current values. There are built-in routines monitoring the emission profile of guns to help keep these calibrations relevant, especially on cold FEG emission guns.

Normalization of dose measurements between microscopes and automated tracking of a sample's beam exposure are critical functions of the MVS software, as they allow quantitative comparisons of dose conditions between experiments to be performed on different microscope systems. Dose induced degradation of a zeolite sample (ZSM-5), obtained during identical experiments using different microscopes, results in complete disappearance of the FFT spots after a maximum cumulative or threshold electron dose ( $\sim 60.000 \text{ e}^-/\text{\AA}^2$  when applying a dose rate of  $\sim 500 \text{ e}^-/\text{\AA}^2 \cdot \text{s}$ ) for both setups. These comparative results demonstrate that the dose software facilitates reproducible, quantitative dose measurements. The small difference in the

cumulative dose at which full FFT spot disappearance is observed for each experiment is likely a result of the different acceleration voltages employed by the two microscopes, with lower acceleration voltages resulting in more radiation damage pathways, and higher acceleration voltages typically resulting in more knock-on damage<sup>24</sup>. Literature results for the critical dose of ZSM-5 nanoparticles range from 9,000-14,000  $e^-/\text{\AA}^2$  using the first FFT spot disappearances, rather than the complete disappearance of all the FFT spots<sup>25,26</sup>. In our results, the first FFT spot disappearance corresponds to a cumulative dose of around 25,000  $e^-/\text{\AA}^2$ . Previous studies relied on current measurements obtained using a phosphor screen, which is well documented to underestimate beam current measurements when compared to a Faraday cup<sup>15</sup>. The determined critical dose can vary by a factor of two or more, depending on which FFT peak is used to track the dose. This indicates that the higher spatial frequencies degrade first, and can result in different values depending on the zone access used during the measurements (our results focused on FFT spots from the entire zeolite crystal, rather than specific structural

features)<sup>25,26</sup>. These differences in techniques and current calibration account for the difference in values between the two experiments reported in our results and previous literature studies.

Although the electron dose interactions are a significant factor in many TEM experiments, *in situ* and specifically liquid-EM studies are particularly sensitive to its effects. Radiolysis of liquids by the electron beam results in a cascade of chemically reactive species which can interact with the sample, complicating the analysis. Both the dose rate or fluence used during a liquid-EM experiment and the cumulative dose can have an influence on the concentration of radical species generated due to liquid radiolysis<sup>27,28</sup>. Thus, collecting and recording both cumulative dose and dose rate metadata throughout an experiment allows direct correlation between images and a sample's dose history, and is a more accurate way to elucidate and control the impact of the electron beam in these experiments. Although not covered in this protocol, an example of the utility of the dose management features for liquid-EM is shown in **Figure 6**.

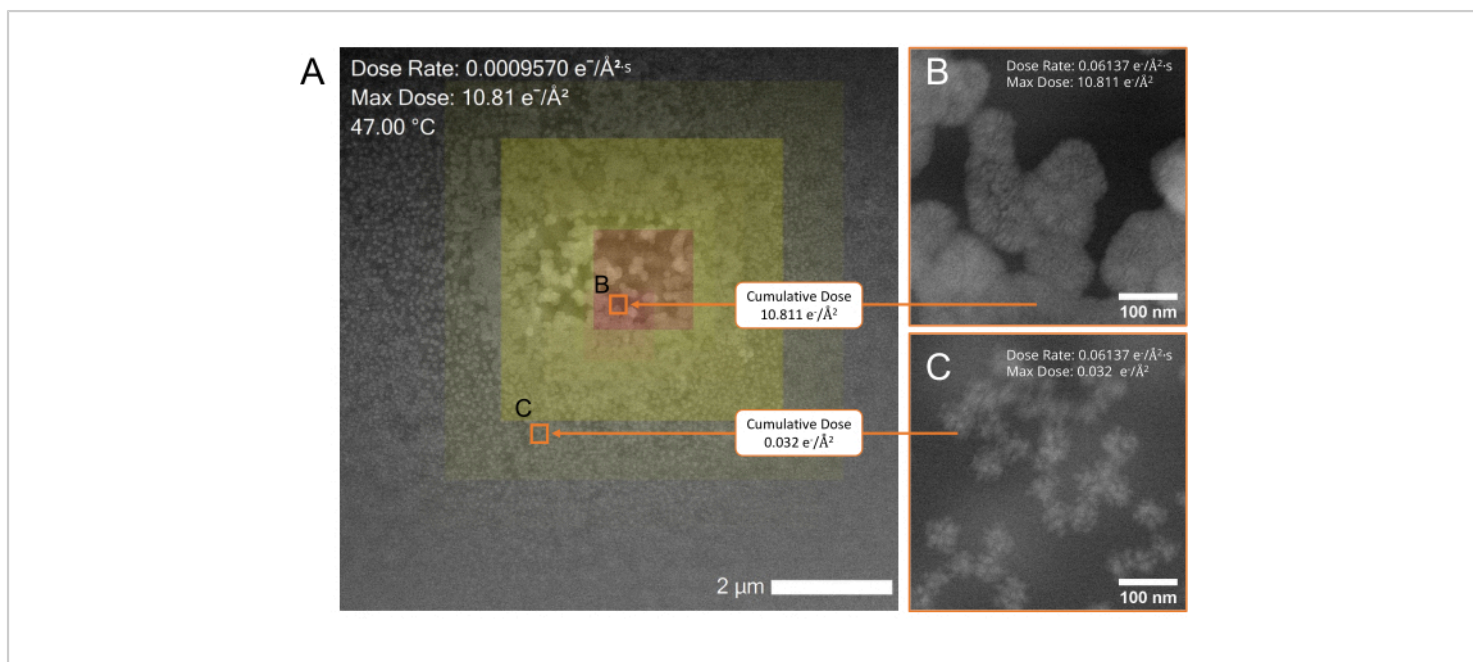


**Figure 6: Beam-induced growth of gold nanoparticles during an *in situ* liquid-EM experiment.** (A) Low-magnification STEM overview of the resulting particle growth with a color overlay of the cumulative dose map across the region. Red areas in the overlay indicate regions of high cumulative dose exposure and yellow areas indicate regions of lower exposure. Highlighting an individual pixel with the cursor or drawing a box over an area using the included drawing tools indicates the cumulative dose for that pixel or area. The scale bar is 2 μm. (B,C) Higher magnification STEM images of the areas indicated by the orange boxes (b,c) in A. Area b, exposed to a higher cumulative dose (10.811 e<sup>-</sup>/Å<sup>2</sup>) contains larger particles than those found in area c, which was exposed to a lower cumulative dose (0.032 e<sup>-</sup>/Å<sup>2</sup>). [Please click here to view a larger version of this figure.](#)

The enriched dose rate and cumulative dose metadata simplifies the analysis of dose-dependent nanomaterial growth and degradation pathways. **Figure 6** shows the beam-induced reduction of a solution of gold auric chloride (HAuCl<sub>3</sub>) ions in water during liquid-EM experiments. From the color dose map overlay in **Figure 6A**, it is easy to visualize that the cumulative electron dose influences the resulting size and shape of the nanoparticles<sup>29,30,31,32</sup>. The low magnification STEM overview shows regions exposed to a high (red) and low (yellow) cumulative dose. The particles in the region exposed to higher doses are larger than those

in the regions exposed to lower cumulative doses. Because the dose metadata is directly embedded in each image at the pixel level, the complex effects of electron dose in liquid-EM experiments can now be systematically analyzed in a way that was never-before achievable.

In this protocol, we have demonstrated that MVS software provides a comprehensive solution for calibrating, monitoring, and tracking both the electron dose and the total dose delivered to a sample on a pixel-by-pixel basis. This ability unlocks a new paradigm for imaging dose-sensitive samples and understanding the electron beam interactions. It is

particularly exciting for liquid-EM experiments, as it will allow for a more effective interrogation into the role that electron dose plays and improve experimental reproducibility. It is our hope that this new framework will allow the accurate collection of dose rate and accumulated dose information, facilitate sharing this data with the community for a more accurate interpretation of TEM results, and advance scientific collaboration and data sharing by enabling FAIR principal reporting and analysis.

## Disclosures

All authors are employees of Protochips, Inc.

## Acknowledgments

This work was performed in part at the Analytical Instrumentation Facility (AIF) at North Carolina State University, which is supported by the State of North Carolina and the National Science Foundation (award number ECCS-2025064). The AIF is a member of the North Carolina Research Triangle Nanotechnology Network (RTNN), a site in the National Nanotechnology Coordinated Infrastructure (NNCI). The authors would like to thank Damien Alloyeau, CNRS Research Director at the University Paris Cité, for providing the 200 kV CFEG zeolite dose threshold study results.

## References

1. Thomas, J. M., Leary, R. K., Eggeman, A. S., Midgley, P. A. The rapidly changing face of electron microscopy. *Chemical Physics Letters*. **631 - 632**, 103-113 (2015).
2. Spurgeon, S. R. et al. Towards data-driven next-generation transmission electron microscopy. *Nature Materials*. **20** (3), 274-279 (2021).
3. Gai, P. L., Boyes, E. D. *In situ* visualisation and analysis of dynamic single atom processes in heterogeneous catalysts. *Journal of Materials Chemistry A*. **10** (11), 5850-5862 (2022).
4. Zheng, H., Lu, X., He, K. In situ transmission electron microscopy and artificial intelligence enabled data analytics for energy materials. *Journal of Energy Chemistry*. **68**, 454-493 (2022).
5. Topsøe, H. Developments in operando studies and in situ characterization of heterogeneous catalysts. *Journal of Catalysis*. **216** (1), 155-164 (2003).
6. Wilkinson, M. D. et al. The FAIR Guiding Principles for scientific data management and stewardship. *Scientific Data*. **3** (1), 160018 (2016).
7. Go Fair. *FAIR Principles*. at <<https://www.go-fair.org/fair-principles/>> (2023).
8. Draxl, C., Scheffler, M. NOMAD: The FAIR concept for big data-driven materials science. *MRS Bulletin*. **43** (9), 676-682 (2018).
9. Kelly, D. F. et al. Liquid-EM goes viral-visualizing structure and dynamics. *Current Opinion in Structural Biology*. **75**, 102426 (2022).
10. Protochips, Inc. *AXON Studio Software Download*. at <[https://success.protochips.com/s/?language=en\\_US](https://success.protochips.com/s/?language=en_US)> (2023).
11. Egerton, R. F., Li, P., Malac, M. Radiation damage in the TEM and SEM. *Micron*. **35** (6), 399-409 (2004).
12. Grubb, D. T. Radiation damage and electron microscopy of organic polymers. *Journal of Materials Science*. **9** (10), 1715-1736 (1974).
13. Buban, J. P., Ramasse, Q., Gipson, B., Browning, N. D., Stahlberg, H. High-resolution low-dose scanning

- transmission electron microscopy. *Journal of Electron Microscopy*. **59** (2), 103-112 (2010).
14. Chen, Q. et al. Imaging beam-sensitive materials by electron microscopy. *Advanced Materials*. **32** (16), 1907619 (2020).
  15. Krause, F. F. et al. Precise measurement of the electron beam current in a TEM. *Ultramicroscopy*. **223**, 113221 (2021).
  16. Žak, A. Guide to controlling the electron dose to improve low-dose imaging of sensitive samples. *Micron*. **145**, 103058 (2021).
  17. Damiano, J. et al. AXON dose: A solution for measuring and managing electron dose in the TEM. *Microscopy Today*. **30** (4), 22-25 (2022).
  18. Allard, L. F., Flytzani-Stephanopoulos, M., Overbury, S. H. Behavior of Au species in Au/Fe<sub>2</sub>O<sub>3</sub> catalysts characterized by novel *in situ* heating techniques and aberration-corrected STEM imaging. *Microscopy and Microanalysis*. **16** (4), 375-385 (2010).
  19. Sze, C., Gulari, E., Demczyk, B. G. Structure of coprecipitated gold-iron oxide catalyst materials. *Materials Letters*. **36** (1-4), 11-16 (1998).
  20. DiCecco, L. A. et al. Advancing high-resolution imaging of virus assemblies in liquid and ice. *Journal of Visualized Experiments*. (185), e63856 (2022).
  21. Dukes, M. J., Gilmore, B. L., Tanner, J. R., McDonald, S. M., Kelly, D. F. In situ TEM of biological assemblies in liquid. *Journal of Visualized Experiments*. (82), e50936 (2013).
  22. Scheutz, G. M. et al. Probing thermoresponsive polymerization-induced self-assembly with variable-temperature liquid-cell transmission electron microscopy. *Matter*. **4** (2), 722-736 (2020).
  23. Howe, J. Y., Allard, L. F., Bigelow, W. C., Demers, H., Overbury, S. H. Understanding catalyst behavior during in situ heating through simultaneous secondary and transmitted electron imaging. *Nanoscale Research Letters*. **9** (1), 614 (2014).
  24. Egerton, R. F. Mechanisms of radiation damage in beam-sensitive specimens, for TEM accelerating voltages between 10 and 300 kV. *Microscopy Research and Technique*. **75** (11), 1550-1556 (2012).
  25. Yoshida, K., Sasaki, Y. Optimal accelerating voltage for HRTEM imaging of zeolite. *Microscopy*. **62** (3), 369-375 (2013).
  26. Yoshida, K., Sasaki, Y., Kurata, H. High-resolution imaging of zeolite with aberration-corrected transmission electron microscopy. *AIP Advances*. **3** (4), 042113 (2013).
  27. Lee, J., Nicholls, D., Browning, N. D., Mehdi, B. L. Controlling radiolysis chemistry on the nanoscale in liquid cell scanning transmission electron microscopy. *Physical Chemistry Chemical Physics*. **23** (33), 17766-17773 (2021).
  28. Schneider, N. M. et al. Electron-water interactions and implications for liquid cell electron microscopy. *The Journal of Physical Chemistry C*. **118** (38), 22373-22382 (2014).
  29. Fritsch, B. et al. Radiolysis-driven evolution of gold nanostructures - model verification by scale bridging in situ liquid-phase transmission electron microscopy and x-ray diffraction. *Advanced Science*. **9** (25), e2202803 (2022).

30. Alloyeau, D. et al. Unravelling kinetic and thermodynamic effects on the growth of gold nanoplates by liquid transmission electron microscopy. *Nano Letters*. **15** (4), 2574-2581 (2015).
31. Ahmad, N., Le Bouar, Y., Ricolleau, C., Alloyeau, D. Growth of dendritic nanostructures by liquid-cell transmission electron microscopy: a reflection of the electron-irradiation history. *Advanced Structural and Chemical Imaging*. **2** (1), 9 (2016).
32. Zhang, Y., Keller, D., Rossell, M. D., Erni, R. Formation of Au nanoparticles in liquid cell transmission electron microscopy: From a systematic study to engineered nanostructures. *Chemistry of Materials*. **29** (24), 10518-10525 (2017).